J. Fluid Mech. (1987), *vol.* 177, *pp.* 395–405
Printed in Great Britain

A conformal-mapping technique for topographic-wave problems: semi-infinite channels and elongated basins

By E. R. JOHNSON†
JISAO, University of Washington, Seattle, WA 98195, USA

(Received 27 May 1986)

The basis of the conformal-mapping method for topographic-wave problems of Johnson (1985) is discussed in greater detail by considering the invariance under conformal mapping of the linear, barotropic, potential-vorticity equation, noted in Davis (1983). A method is presented for using this property to construct further solutions for waves propagating over varying topography. Results are given for semi-infinite channels and elongated basins. A coordinate system is constructed that approaches a Cartesian system exponentially fast with distance from end-walls. For exponentially sloping topography the solutions for infinite channels, semi-infinite channels, and basins have the same structure and dispersion relation as waves in an elliptical basin, discussed in Johnson (1987). The structures presented there can thus be considered as in some sense universal for exponentially sloping topography.

1. Introduction

In a recent paper (Johnson 1985), a conformal-mapping method was introduced to transform the problem of topographic waves approaching a cross-step wall into that of waves propagating along a channel, from which a solution followed directly. The present work discusses the basis of this method in greater detail and presents examples for topographic waves in semi-infinite channels and elongated basins.

In §2 a brief derivation is given of the result that the barotropic, rigid-lid, topographic wave equation is invariant under conformal mappings, a property noted by Davis (1983). The vast classical literature on conformal mappings is thus available for solving topographic wave problems in various geometries. The relationship of this result to that of Rhines & Bretherton (1973), on depth profiles for which the topographic wave equation reduces to Helmholtz's equation, is discussed.

Section 3 presents briefly the structure of topographic waves in a symmetric infinite channel. The dispersion relation for topography varying exponentially across the channel and constant along the channel is precisely that for topographic waves in an elliptical basin, given in Johnson (1987) (called I hereinafter). Waves propagate in both directions along the channel, being concentrated above the slope favourable to their direction of propagation (i.e. with shallow water to their right). The topographic wave structure and dispersion relations of I are thus in some sense universal, as is borne out in the following sections.

The example chosen to illustrate use of the conformal property is introduced in §4, which considers the problem of waves propagating in a semi-infinite channel. It

† Permanent address: Department of Mathematics, University College London, Gower Street, London, WC1E 6BT, UK.

is shown that the semi-infinite channel can be mapped conformally onto the infinite symmetric channel of §3. Although more general depth variations can be considered, attention is restricted to depth profiles exponentially varying in the cross-channel coordinate and independent of the along-channel coordinate for which the topographic wave equation has constant coefficients. The conformal-mapping method has generated bottom topography satisfying the Rhines & Bretherton (1973) criterion, see (2.4) below. Results in I show the necessity of considering waves propagating in both directions and the derived cross-channel structures and dispersion relation are precisely those of I, once allowance is made for the renamed coordinates. Topographic waves propagating into the channel concentrated against one wall move towards the channel end where they are smoothly turned to propagate out against the opposite wall. The coordinate system chosen for the semi-infinite channel approaches exponentially fast the Cartesian system for an infinite channel and thus closed-basin solutions are obtained in §5 by reflections about the channel centreline and open boundary and judicious choice of the along-channel wavenumber. For a basin of length/width ratio of 2 this introduces an error of less than 0.2 % and in the presented examples, with an aspect ratio of 6, the error is of order e^{-40}. Section 6 contains some general results following from the analysis and a brief comparison of predicted periods with those observed in intermontane lakes.

2. Invariance principle

The non-dimensional linear barotropic potential-vorticity equation can be written (Rhines 1969) as

$$\nabla\cdot(h^{-1}\nabla\psi_t)+(\nabla\psi\wedge\nabla h^{-1})\cdot\hat{\boldsymbol{z}}=0, \tag{2.1}$$

where h is the depth, $\hat{\boldsymbol{z}}$ a unit vector along the axis of rotation and ψ the depth-independent mass-transport stream function. Perhaps the simplest demonstration of invariance follows by continuing the analysis of Mysak (1985). Introduce curvilinear coordinates (x_1, x_2, z), with corresponding scale factors $(h_1, h_2, 1)$. Then (2.1) becomes

$$\frac{\partial}{\partial x_1}\left(\frac{h_2}{hh_1}\frac{\partial^2\psi}{\partial x_1\,\partial t}\right)+\frac{\partial}{\partial x_2}\left(\frac{h_1}{hh_2}\frac{\partial^2\psi}{\partial x_2\,\partial t}\right)+\frac{\partial\psi}{\partial x_1}\frac{\partial h^{-1}}{\partial x_2}-\frac{\partial\psi}{\partial x_2}\frac{\partial h^{-1}}{\partial x_1}=0. \tag{2.2}$$

For any coordinate system (x_1, x_2) obtained by conformal mapping from Cartesian coordinates (x, y), the Cauchy–Riemann equations imply that the scale factors h_1 and h_2 are equal, and (2.2) becomes

$$\frac{\partial}{\partial t}\left(\frac{\partial^2\psi}{\partial x_1^2}+\frac{\partial^2\psi}{\partial x_2^2}\right)-\frac{\partial}{\partial x_1}\log h\left(\frac{\partial^2\psi}{\partial x_1\,\partial t}-\frac{\partial\psi}{\partial x_2}\right)-\frac{\partial}{\partial x_2}\log h\left(\frac{\partial^2\psi}{\partial x_2\,\partial t}+\frac{\partial\psi}{\partial x_1}\right)=0. \tag{2.3}$$

The topographic wave equation is invariant under conformal mappings. This is the property used in Johnson (1985) and includes the elliptical coordinates discussed by Mysak (1985), who considers $h = h(x_1)$ so that the final term in (2.3) is absent. It appears that this property was first noted by Davis (1983) when discussing shelf-similar topographies.

Rhines & Bretherton (1973) note an alternative reduction of the topographic wave equation (2.3), to a Helmholtz equation with non-constant wavenumber, valid whenever the topography satisfies

$$\nabla^2(\log h)=0. \tag{2.4}$$

Davis (1983) presents a different derivation of this result. The conformal-mapping invariance differs significantly from the Helmholtz reduction as it requires no restriction on the topography considered, and so is useful in numerical solutions in unusual geometries. However, in analytical applications it appears most useful to consider topographies for which (2.3) has constant coefficients, i.e. $\log h$ is a linear function of x_1 and x_2 and so satisfies (2.4). The example in §4 is of this form.

3. Infinite symmetric channel

Consider the channel $|y| \leqslant y_s$, $-\infty < x < \infty$ with a depth profile independent of position along the channel (i.e. $h = h(y)$ alone). Equation (2.3) reduces to

$$h^{-1}\psi_{xxt} + (h^{-1}\psi_{yt})_y + (h^{-1})_y \psi_x = 0. \tag{3.1}$$

Restricting consideration to flows with no flux along the channel gives the boundary conditions

$$\psi = 0 \quad (y = \pm y_s). \tag{3.2}$$

For even h, i.e. symmetric channels, (3.1) is invariant under the transformation $(x, y, t) \to (x, -y, -t)$, and so for each wave propagating in the positive x-direction there is an identical wave propagating in the negative x-direction, related to the first by reflection about the channel centreline.† Thus look for a solution of (3.1) corresponding to a wave propagating in the positive x-direction, i.e.

$$\psi_1 = \mathrm{Re}\{F(y) \exp(\mathrm{i}\sigma t - \mathrm{i}kx)\}, \tag{3.3}$$

with σ and k positive, noting that the reflection,

$$\psi_2 = \mathrm{Re}\{F(-y) \exp(\mathrm{i}\sigma t + \mathrm{i}kx)\}, \tag{3.4}$$

is then a solution corresponding to a wave propagating in the negative x-direction. The cross-channel function F satisfies

$$(h^{-1}F')' + [k\sigma^{-1}(h^{-1})' - k^2 h^{-1}]F = 0 \quad (0 \leqslant |y| \leqslant y_s), \tag{3.5}$$

$$F(y_s) = 0, \quad F(-y_s) = 0. \tag{3.6a, b}$$

The form of the linear eigenvalue problem (3.5), (3.6) allows F to be taken as purely real and so (3.3) and (3.4) reduce to

$$\psi_1 = F(y)\cos(kx - \sigma t), \quad \psi_2 = F(-y)\cos(kx + \sigma t). \tag{3.7a, b}$$

As a simple example, consider the exponential depth profile

$$h = \begin{cases} 1 & (|y| \leqslant y_b) \\ \exp[-b(|y| - y_b)] & (y_b \leqslant |y| \leqslant y_s). \end{cases} \tag{3.8}$$

Then (2.5) reduces to the standard shelf-wave equations

$$\left.\begin{aligned} F'' \pm bF' + \left(\pm\frac{kb}{\sigma} - k^2\right)F = 0 \quad (y_s > \pm y > y_b), \\ F'' - k^2 F = 0 \quad (|y| \leqslant y_b). \end{aligned}\right\} \tag{3.9}$$

† It can be shown that propagation in both directions occurs in any channel whose depth increases monotonically from the banks to some central maximum; however, the more restricted case is sufficient for the present illustration.

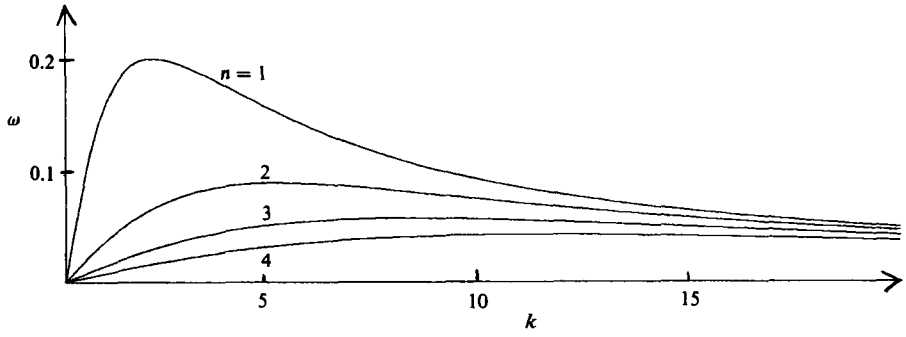

FIGURE 1. The dispersion relation giving frequency as a function of along-channel wavenumber for a channel of half-width $y_s = 1.5$, with flat-bottomed central section, $|y| \leqslant y_b = 0.5$, and logarithmic slope $b = 1$.

The boundary conditions on (3.9) are (3.6) and the requirement that ψ and its normal derivative are continuous at $|y| = y_b$. Hence the cross-stream structure is given by

$$F = \begin{cases} \left[\cosh ky_b + \frac{\alpha_1}{k}\sinh ky_b\right]^{-1} \dfrac{\exp\left[-\frac{1}{2}b(y-y_b)\right]\sin\left[\lambda_1(y_s-y)\right]}{\sin\left[\lambda_1(y_s-y_b)\right]} & (y_b < y < y_s) \\ \cosh ky - (k\tanh ky_b + \alpha_1)(k+\alpha_1\tanh ky_b)^{-1}\sinh ky & (|y| < y_b) \\ \left[\cosh ky_b + \frac{\alpha_2}{k}\sinh ky_b\right]^{-1} \dfrac{\exp\left[-\frac{1}{2}b(y+y_b)\right]\sinh\left[\lambda_2(y+y_s)\right]}{\sinh\left[\lambda_2(y_s-y_b)\right]}, & (-y_s < y < -y_b), \end{cases} \tag{3.10}$$

where

$$\alpha_1 = \lambda_1 \cot\left[\lambda_1(y_s-y_b)\right] + \tfrac{1}{2}b, \tag{3.11a}$$

$$\alpha_2 = \lambda_2 \coth\left[\lambda_2(y_s-y_b)\right] + \tfrac{1}{2}b, \tag{3.11b}$$

$$\lambda_1^2 = \frac{kb}{\sigma} - k^2 - \tfrac{1}{4}b^2, \quad \lambda_2^2 = \frac{kb}{\sigma} + k^2 + \tfrac{1}{4}b^2, \tag{3.12a, b}$$

the arbitrary amplitude has been chosen so that $F(0) = 1$, and λ_1 satisfies the eigenvalue relation $G(\lambda_1) = 0$ where

$$G(\lambda_1) = (\alpha_1+\alpha_2)(1+\tanh^2 ky_b) + 2\left(k + \frac{\alpha_1\alpha_2}{k}\right)\tanh ky_b. \tag{3.13}$$

The structure of this solution is the same as that given in I. The solutions differ solely because the curving end of the elliptic basin requires both leftward- and rightward-propagating waves to be present simultaneously and because periodicity in the basin restricts the alongshore wavenumber k to integral values. Both of these effects are dealt with in the following sections.

Once λ_1 is obtained from (3.13), the corresponding frequency follows from (3.12a), which implies the upper bound

$$\sigma < \frac{kb}{k^2 + \frac{1}{4}b^2}.$$

As noted in I, these relations take a particularly simple form when the flat-bottomed section is absent from the channel (i.e. $y_b = 0$). In particular, (3.13) reduces to

$$G(\lambda_1) = \alpha_1 + \alpha_2, \tag{3.14}$$

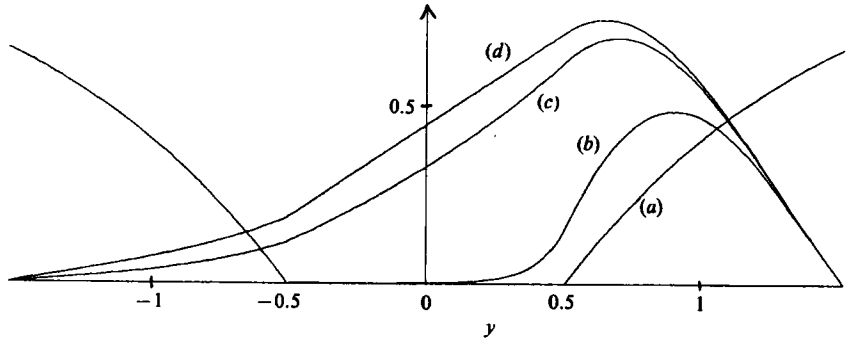

FIGURE 2. Cross-channel structure of the infinite-channel solutions for the parameter values of figure 1. (*a*) The depth profile, $1-h$, with h given by (3.8). The fundamental mode structure, normalized to have unit negative slope at y_s, for along-channel wavenumbers (*b*) $k = 10$, (*c*) $k = 1$ and (*d*) $k = 0.1$.

and it follows that for each k there are countably many eigenvalues $\lambda_1^{(n)}$ that satisfy

$$(n-\tfrac{1}{2})\pi < y_s \lambda_1^{(n)} < n\pi \quad (n = 1, 2, 3, \ldots), \tag{3.15a}$$

$$y_s \lambda_1^{(n)} \to (n-\tfrac{1}{4})\pi \quad (n, k, \text{ or } y_s \text{ large}). \tag{3.15b}$$

The solutions allowing for the flat bottom are, however, sufficiently straightforward to be discussed directly and certainly allow a closer matching of model topography with actual channel profiles.

Figure 1 gives a graph of the dispersion relation for parameters $y_s = 1.5$, $y_b = 0.5$, and $b = 1$, corresponding to a channel depth profile whose central third is flat. The graph resembles standard shelf-wave dispersion relations with long waves non-dispersive, short waves dispersive and zero group velocity at some finite alongshore wavenumber. For a given alongshore wavenumber, the fundamental mode has the shortest period. The shortest period for a given wave occurs for waves and slopes such that the total wavenumber and b are of the same order.

Figure 2 gives the depth profile for these parameter values and the cross-channel structure of the fundamental mode for various along-channel wavenumbers. In each case the wave is concentrated on the channel side that lies to the right of the direction of propagation – the shorter the along-channel wavelength the greater the confinement. The wave decays away from the slope region favourable to its direction of propagation.

4. Semi-infinite channel

Consider the semi-infinite channel $|y| < \frac{1}{2}\pi$, $x \geqslant 0$ with a cut on $y = 0$, $(x \geqslant a)$ as shown in figure 3(*a*). The transformation

$$\sigma + i\tau = \sinh(x + iy) \tag{4.1}$$

maps this region onto the half-plane $\sigma \geqslant 0$ with the cut on $\tau = 0$ $(\sigma \geqslant \sinh a)$, shown in figure 3(*b*). The further transformation

$$\xi + i\eta = \cosh^{-1}\frac{\sigma + i\tau}{\sinh a} = \cosh^{-1}\frac{\sinh(x + iy)}{\sinh a} \tag{4.2}$$

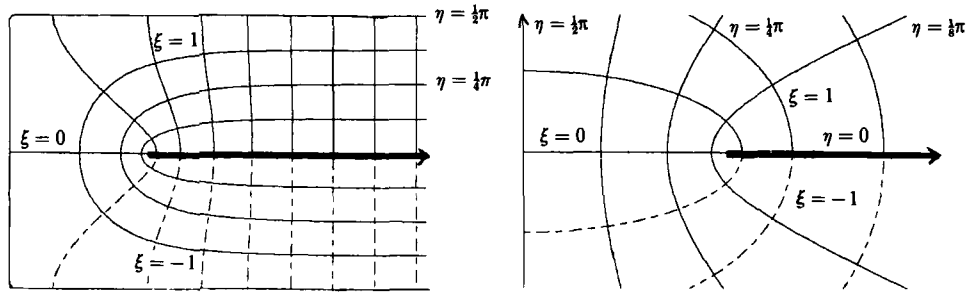

FIGURE 3. (*a*) The semi-infinite channel $|y| \leqslant \frac{1}{2}\pi$, $x \geqslant 0$. Isolines of the (ξ, η)-coordinate system defined by $\xi + i\eta = \cosh^{-1}[\sinh(x+iy)/\sinh a]$ are included with negative values dashed. The cut along $y = 0$ for $x \geqslant a$ is shown thickened. Here $a = \frac{1}{2}\pi$. (*b*) The half-plane $\sigma \geqslant 0$ into which the channel of (*a*) transforms under the mapping $\sigma + i\tau = \sinh(x+iy)$. The cut is thickened and isolines of (ξ, η) are included. These are standard elliptic coordinate lines.

maps this half-plane onto the strip $0 \leqslant \eta \leqslant \frac{1}{2}\pi$, $-\infty < \xi < \infty$, and is equivalent to introducing elliptic coordinates through

$$\sigma = (\sinh a)\cosh\xi\cos\eta, \quad \tau = (\sinh a)\sinh\xi\sin\eta. \tag{4.3}$$

Some isolines of ξ and η are included in figure 3. Far from the channel end (i.e. $x \gg 1$), (4.2) reduces to

$$\xi + i\eta = \operatorname{sgn} y\{x + iy - \log(\sinh a) - \cosh^2 a \exp[-2(x+iy)] + \ldots\}. \tag{4.4}$$

Isolines of (ξ, η) differ from those of (x, y) by an amount of order $\exp(-2x)\cosh^2 a$. One channel width from the end, for a of order unity or less, the two systems differ by less than 0.2%. Isolines of (ξ, η) correspond to force lines and equipotentials for a charged semi-infinite plate inside a grounded semi-infinite, closed-end container.

For a depth profile that is a function of η alone (corresponding far from the channel end to the constant-cross-section infinite channel considered in the previous section), the conformal-mapping property of §2 implies that the topographic wave equation has precisely the form (3.1) with (ξ, η) replacing (x, y). The boundary conditions in the present geometry are those of no normal flow through the channel wall and continuity of the stream function and its normal derivative across the cut $\eta = 0$ (since h is continuous there). As pointed out in I, it is necessary to consider waves propagating in both directions, and thus look for solutions of the form

$$\psi = \operatorname{Re}\{F_1(\eta)\exp[i(\sigma t + k\xi)] + F_2(\eta)\exp[i(\sigma t - k\xi)]\} \tag{4.5a}$$

$$= \operatorname{Re}\{\exp(i\sigma t)[(F_1 + F_2)\cos k\xi + i(F_1 - F_2)\sin k\xi]\}, \tag{4.5b}$$

where, without loss of generality, the frequency σ and alongshore wavenumber k can be taken as positive. The cross-channel functions F_1 and F_2 satisfy, as in I,

$$(h^{-1}F')' + [\pm k\sigma^{-1}(h^{-1})' - k^2 h^{-1}]F = 0 \quad (0 < \eta < \eta_s), \tag{4.6}$$

$$F(\eta_s) = 0, \tag{4.7}$$

where the channel boundary has been taken to be the curve $\eta = \eta_s$ $(0 < \eta_s \leqslant \frac{1}{2}\pi)$. The

continuity of ψ and ψ_η across $\eta = 0$ requires, from (4.5b) near $\eta = 0$, that ψ be a symmetric function of ξ and ψ_η antisymmetric. Thus, as in I,

$$F_1'(0)+F_2'(0) = 0, \quad F_1(0)-F_2(0) = 0. \tag{4.8a, b}$$

System (4.6), (4.7), (4.8) is a well-posed linear eigenvalue problem for the frequency σ and the cross-channel structured $F_{1,2}$. Its form allows $F_{1,2}$ to be taken as purely real and so (4.5) reduces to

$$\psi = F_1 \cos(k\xi-\sigma t)+F_2 \cos(k\xi+\sigma t). \tag{4.9}$$

Although the eigenvalue problem can be solved numerically, simply and directly, for arbitrary profiles $h(\eta)$, a standard exponential profile gives much information on the structure of solutions. Consider the profile

$$h = \begin{cases} \exp[-b(\eta-\eta_b)] & (\eta_b \leqslant \eta \leqslant \eta_s) \\ 1 & (0 \leqslant \eta \leqslant \eta_b), \end{cases} \tag{4.10}$$

for $b > 0$, and $\eta_b \geqslant 0$. The exponentially sloping region is confined near the channel walls, the bottom being flat within the region $\eta \leqslant \eta_b$. Far from the endwall this profile reduces to that considered in the previous section. Substituting (4.10) in (4.6) gives constant-coefficient equations in the regions $\eta_b \leqslant \eta \leqslant \eta_s$ and $0 \leqslant \eta \leqslant \eta_b$. The solution of these equations satisfying (4.7), (4.8) and having ψ and ψ_η continuous at $\eta = \eta_b$ is given in I (allowing for the interchange of the roles of ξ and η) as

$$F_1 = \left[\cosh k\eta_b + \frac{\alpha_1}{k}\sinh k\eta_b\right]^{-1}$$

$$\times \begin{cases} \dfrac{\exp[-\frac{1}{2}b(\eta-\eta_b)]\sin[\lambda_1(\eta_s-\eta)]}{\sin[\lambda_1(\eta_s-\eta_b)]} & (\eta_b \leqslant \eta \leqslant \eta_s) \qquad (4.11a) \\ \cosh[k(\eta-\eta_b)]-\dfrac{\alpha_1}{k}\sinh[k(\eta-\eta_b)], & (0 \leqslant \eta \leqslant \eta_b) \qquad (4.11b) \end{cases}$$

$$F_2 = \left[\cosh k\eta_b + \frac{\alpha_2}{k}\sinh k\eta_b\right]^{-1}$$

$$\times \begin{cases} \dfrac{\exp[-\frac{1}{2}b(\eta-\eta_b)]\sinh[\lambda_2(\eta_s-\eta)]}{\sinh[\lambda_2(\eta_s-\eta_b)]} & (\eta_b \leqslant \eta \leqslant \eta_s) \qquad (4.12a) \\ \cosh[k(\eta-\eta_b)]-\dfrac{\alpha_2}{k}\sinh[k(\eta-\eta_b)], & (0 \leqslant \eta \leqslant \eta_b) \qquad (4.12b) \end{cases}$$

where λ_1, λ_2 are defined in the previous section, as are α_1, α_2 once y_s, y_b are replaced by η_s, η_b. The eigenvalue relation is again (3.13), unaltered from I, and the dispersion relation for $\eta_s = 1.5$, $\eta_b = 0.5$, $b = 1$ is given by figure 1. The sole effect, away from the channel end, of the introduction of the end is to force waves propagating in both directions to be present simultaneously. A wave moving to the left down the channel, concentrated against the wall at $y = y_s$, is smoothly turned by the channel end and emerges as a wave moving to the right concentrated against the wall at $y = -y_s$.

Figure 4 gives streamlines of the fundamental mode near the channel end at one-eighth-period intervals for the parameters $\eta_s = 1.5$, $\eta_b = 0.5$, $b = 1$, for which, away from the channel end, the cross-channel structures reduce to those of figure 2. The remaining disposable parameters are the along-channel wavenumber and the

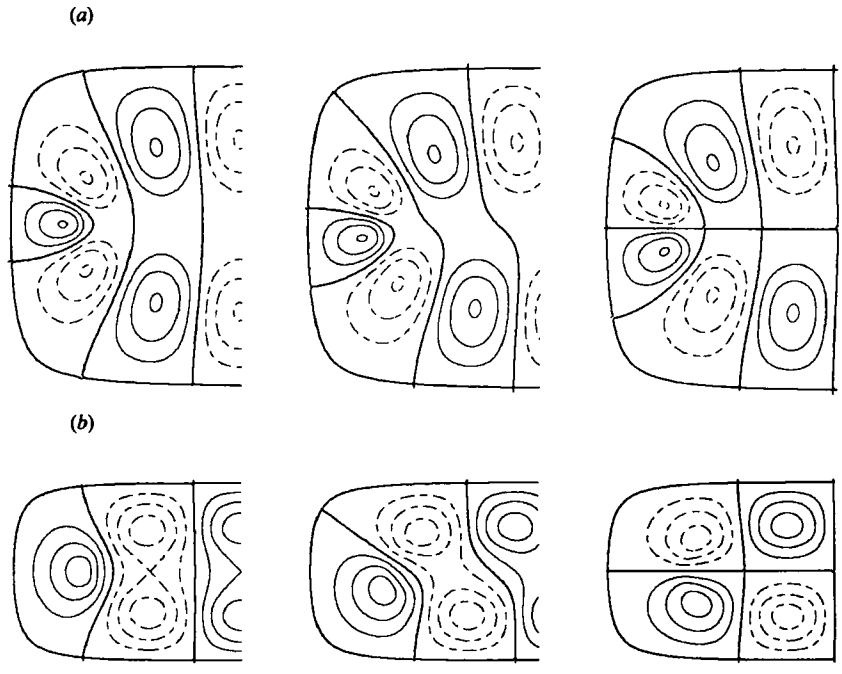

FIGURE 4. Streamlines at one-eighth-period intervals of the fundamental mode near the end of a semi-infinite channel for the parameter values of figure 1. The patterns at later times follow by symmetry. (*a*) Tightly bunched end contours ($a = \frac{1}{4}\pi$), $k = 4$. Waves shorten and slow to squeeze through the narrow gap. (*b*) A smoother channel end ($a = \frac{1}{2}\pi$), $k = 1$. Waves pass smoothly round the endwall. Negative values are dashed and the zero line thickened.

gap parameter a. For small a, waves decrease in wavelength and squeeze slowly through the steep topography of bunched coordinate lines at the channel end. This behaviour is shown in figure 4(*a*) where $a = \frac{1}{4}\pi$ and $k = 4$, and is closely related to the increasing wavenumber and decreasing speed of topographic waves approaching a cross-slope wall, discussed in Johnson (1985). For moderate a, of order the channel width, waves pass smoothly round the channel end without reduction of speed. This is shown in figure 4(*b*) where $a = \frac{1}{2}\pi$ and $k = 2$.

5. Elongated basins

Topographic-wave modes for basins of arbitrary elongation could be found by mapping the basin interior onto a semi-infinite channel. Following the choice of the previous section, a suitable coordinate system could be obtained by considering the force lines and equipotentials for a charged plate inside a grounded box. The usefulness of such an approach in finding explicit solutions is limited as the mapping involves elliptic functions, losing the simplicity of the previous section. Modes for basins of length/width ratio of order unity have, however, been presented in I and so it is sufficient to restrict attention to elongated basins.

The stream function $\psi^{(b)}$ defined in terms of the stream function ψ of the previous section by

$$\psi^{(b)}(x,y) = \begin{cases} \psi(x,y) & (0 \leqslant x \leqslant L), \\ \pm\psi(2L-x,-y) & (L \leqslant x \leqslant 2L), \end{cases} \tag{5.1}$$

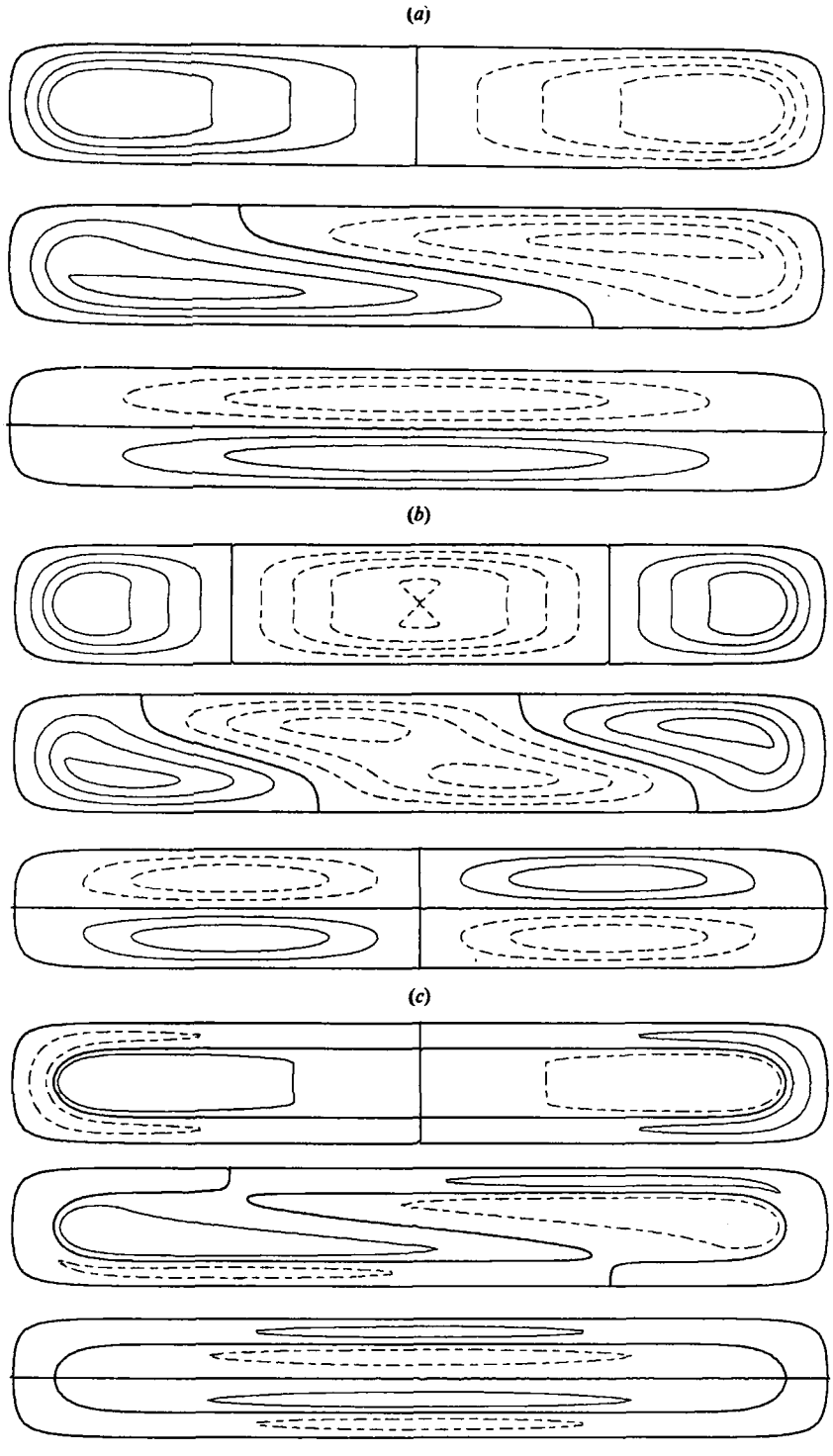

FIGURE 5. Normal modes in a basin for the parameter values of figure 1, and a gap of $a = \frac{1}{2}\pi$. The basin is six times as long as it is wide. (*a*) The fundamental mode, $(m, n) = (1, 1)$; (*b*) $(m, n) = (2, 1)$; (*c*) $(m, n) = (1, 2)$. The region of irrotational flow above the central third of the basin width is clearly visible.

is a solution for a basin of length $2L$ of the topographic-wave equation provided that $\psi^{(b)}$ and $\psi_x^{(b)}$ are continuous at $x = L$. From the discussion of the previous section it follows that the continuity conditions are satisfied with error of order $\exp(-2L)\cosh^2 a$ provided that ψ is periodic in ξ with period a multiple of ξ_L where $\xi_L = L - \log(\sinh a)$. The upper sign in (5.1) corresponds to even multiples and the lower to odd multiples. Equation (4.9) shows that ψ has the required form provided $k = m\pi/2\xi_L$, $m = 1, 2, 3, \ldots$. The inclusion of a second endwall on the channel restricts the long-basin wavenumber to discrete values as in the elliptical basin solutions of I. For a basin twice as long as wide the continuity conditions are satisfied with an error less than 0.2% and this error decreases exponentially with increasing length/width ratio. Reflection about the figure-end and about the line $y = 0$ in figure 4(*a*, *b*) thus generates the modes $(m, n) = (3, 1)$ and $(4, 1)$ respectively for the basins so formed. Figure 5 gives streamlines at one-eighth-period intervals for a basin of length-to-width ratio of 6 (so the continuity conditions are satisfied to order e^{-40}) for the modes $(m, n) = (1, 1)$, $(2, 1)$ and $(1, 2)$.

6. Discussion

The basis of the conformal-mapping method for the topographic-wave problems of Johnson (1985) has been discussed in greater detail by considering the invariance under conformal mappings of the linear, barotropic, potential-vorticity equation, noted in Davis (1983), and the method used to construct solutions corresponding to topographic waves propagating in a semi-infinite channel. The mapping was constructed so that away from the channel end the curvilinear coordinates approached, exponentially fast, standard Cartesian coordinates. This enables closed-basin solutions to be obtained with error decaying exponentially with increasing length/width ratio of the basin. The solutions for infinite channels, semi-infinite channels and basins are of the same structure and have the same dispersion relation as those in I for waves in an elliptical basin with exponentially sloping sides and a flat bottom. The results presented in I are universal for bathymetry that can be mapped conformally onto a semi-infinite channel with exponential topography. The sole effect of differing geometries lies in the precise values of the parameters appearing in the dispersion relation. The invariance property divides topographies into equivalence classes in which members of the same class are related through conformal mappings.

The present results can be applied to estimating topographic periods in elongated intermontane lakes. Previous estimates in Mysak (1985) and I using the elliptical-basin model suffer from the weakness that choosing disposable parameters to model the lake ends at all acurately leads to unrealistic length/width ratios for the basins. The present model removes these difficulties. The four parameters a, b, η_b and η_s are available to model the lake end and, additionally, to prescribe what portion of the central lake region is flat. The basin length is determined independently. The bathymetry of Swiss lakes shown in Mysak (1985) and Mysak *et al.* (1985) indicates that reasonable choices of a, b, η_b and η_s are of order unity. The length-to-width ratio of the lakes is of order 10 and thus the alongshore wavenumber k is of order $0.05m$ for mode numbers $m = 1, 2, \ldots$. Computations from the dispersion relation show that realistic values of wave periods occur only for k of order unity (as it is for the fundamental mode in an elliptical basin, for which periods are calculated in I). This leads to the conjecture that, if the reported oscillations in intermontane lakes are topographic waves, they may correspond to alongshore wavenumbers of order the length/width ratio, and not the fundamental mode as conjectured in Mysak (1985).

This work was undertaken during a sabbatical visit to the University of Washington, supported in part by grant NA85ABH00031 from the U.S. Department of Commerce and grant OCE84-45194 from the National Science Foundation. It is a pleasure to acknowledge the kind hospitality of both the Joint Institute for the Study of the Atmosphere and Ocean and the Department of Applied Mathematics. Contribution no. 32, JISAO (May 1986).

REFERENCES

DAVIS, A. M. J. 1983 Shelf similar topographies for free continental shelf waves. *Geophys. Astrophys. Fluid Dyn.* **23**, 321–331.

JOHNSON, E. R. 1985 Topographic waves and the evolution of coastal currents. *J. Fluid Mech.* **160**, 499–509.

JOHNSON, E. R. 1987 Topographic waves in elliptical basins. *Geophys. Astrophys. Fluid Dyn.* **37**, 279–296.

MYSAK, L. A. 1985 Elliptical topographic waves. *Geophys. Astrophys. Fluid Dyn.* **31**, 93–135.

MYSAK, L. A., SALVADE, G., HUTTER, K. & SCHEIWILLER, T. 1985 Topographic waves in a stratified elliptical basin, with application to the Lake of Lugano. *Phil. Trans. R. Soc. Lond.* **A316**, 1–55.

RHINES, P. B. 1969 Slow oscillations in an ocean of varying depth. Part 2. Islands and seamounts. *J. Fluid Mech.* **37**, 191–105.

RHINES, P. B. & BRETHERTON, F. 1973 Topographic Rossby waves in a rough-bottomed ocean. *J. Fluid Mech.* **61**, 583–607.